Thermal conductance boost in phononic crystal nanostructures

Roman Anufriev[1] and Masahiro Nomura[1,2,*]

[1]*Institute of Industrial Science, the University of Tokyo, Tokyo, 153-8505, Japan*

[2]*Institute for Nano Quantum Information Electronics, the University of Tokyo, Tokyo, 153-8505, Japan*

(Received 13 April 2015; revised manuscript received 22 May 2015; published 15 June 2015)

A theoretical study of coherent phonon scattering in thin-film phononic-crystal nanostructures (also called thermocrystals) is presented. It is commonly assumed that phononic crystals may only reduce thermal conductivity of materials. In this theoretical paper, contrary to this assumption, we demonstrate that phononic nanopatterning can enhance the thermal conductance of thin films under certain conditions. That is to say, it is shown that a thin membrane with many holes can have a higher thermal conductance than an unpatterned membrane. This effect originates from the increase in the density of states due to the coherent modifications of phonon dispersion. This counterintuitive phenomenon, called the thermal conductance boost effect, can be used for applications involving phonon management.

DOI: 10.1103/PhysRevB.91.245417 PACS number(s): 63.22.−m, 63.20.D−, 66.70.−f

Phononic crystals are artificially periodic metamaterials where the dispersion relation of elastic waves is affected by Bragg diffraction. Due to the wave nature of phonons, the phononic crystals can be used to control the phonon transport, which makes phononic nanostructures potential candidates for various applications involving phonon management [1–3]. Indeed, the phonon group velocity [4–6] and the density of states (DOS) [5,7,8] can be modified by the periodicity of the media. This phenomenon, known as coherent scattering, is often regarded as one of the mechanisms that reduce the thermal conductivity of nanostructures [6,7,9]. However, at room temperature the thermal conductivity is mostly controlled by other scattering mechanisms, referred to as incoherent scattering [10–15]. Nevertheless, recent experiments on two-dimensional (2D) phononic crystals demonstrated that at sub-Kelvin temperatures the thermal conductance of a structure with a higher surface to volume ratio was greater than that of a structure with a lower ratio [5]. This counterintuitive result could not be explained in terms of incoherent scattering mechanisms and was attributed to the coherent modifications of phonon dispersion that reduce the group velocity and the DOS. This shows that wave properties of phonons may play a key role in heat transport, which can therefore be controlled by the design of phononic crystals. However, periodic patterning with air holes is commonly known to reduce thermal conductance of patterned structures as compared to unpatterned ones due to the fact that holes efficiently scatter phonons from both coherent and incoherent points of view [5,9,11,15]. In this paper, we adopt the theoretical approach of Ref. [5] to demonstrate that, under certain conditions, changes in the phonon dispersion may, on the contrary, lead to the enhancement of thermal conductance of patterned structures as compared to unpatterned ones. This thermal conductance boost effect is strongly temperature dependent and can be controlled via the design of the phononic crystal, allowing for its use in applications involving phonon management.

We consider ideal 2D silicon thin-film phononic crystals with hexagonal air-hole lattices [Fig. 1(a)]. To simulate infinite periodic arrays of holes in thin freestanding films (membranes), we model a three-dimensional unit cell of finite thickness with Floquet periodic boundary conditions on the x-y plane [16]. In the low-temperature limit, the phonon wavelength is longer than the characteristic scale of the system, thus we can use the classical elasticity theory to compute the phonon dispersion. We use the finite element method (FEM), implemented by COMSOL MULTIPHYSICS® v4.4 software, to numerically calculate the eigenfrequencies from the elastodynamic wave equation $\mu\nabla^2\mathbf{u} + (\mu+\lambda)\nabla(\nabla\cdot\mathbf{u}) = -\rho\omega^2\mathbf{u}$, where $\mathbf{u}$ is the displacement vector, ρ is the mass density, and λ and μ are Lamé parameters of silicon. Bloch's theorem guarantees the existence of the solutions $\mathbf{u}(k)$ in the form of a plane wave with the eigenfrequencies $\omega(k)$. First we calculate the eigenfrequencies for the wave vectors at the periphery (mesh consists of 500 nods) of the irreducible triangle of the first Brillouin zone (BZ) [Fig. 1(b)]. Figure 1(c) shows the obtained band diagram for a typical hexagonal lattice structure with thickness (h) and period (a) equal to 80 nm and hole radius to period ratio (r/a) equal to 0.4. Then we obtain the eigenfrequencies in the interior of the BZ as an extrapolation with careful attention to the intersection of the branches [Fig. 1(c)]. To study the heat transport we calculate the frequency spectra of the heat flux. First we calculate the values of the group velocity $v_{\mathrm{gr}}(\omega) = \nabla\omega(k)$ averaged between all values corresponding to the given frequency over the entire BZ. The energy density of phonons is $\hbar\omega\cdot D(\omega)$, where $D(\omega)$ is the DOS—the number of states per unit volume is given by

$$D(\omega) = \sum_m \int_l \frac{dl}{\nabla\omega_m(k)}, \tag{1}$$

where the integral of l gives the length of constant frequency in k space and m is the number of the mode [17]. At a given temperature only a certain number of states is available, thus the energy density should be weighted by the Bose-Einstein distribution $n(\omega,T)$. Finally, neglecting the size of the heater, the heat flux $Q(\omega,T)$ is proportional to $\hbar\omega\cdot D(\omega)\cdot v_{\mathrm{gr}}(\omega)\cdot n(\omega,T)$.

In this paper we compare the data obtained for phononic-crystal membranes to that of an unpatterned membrane of the same thickness. To obtain the membrane dispersion, we

*Email address: nomura@iis.u-tokyo.ac.jp

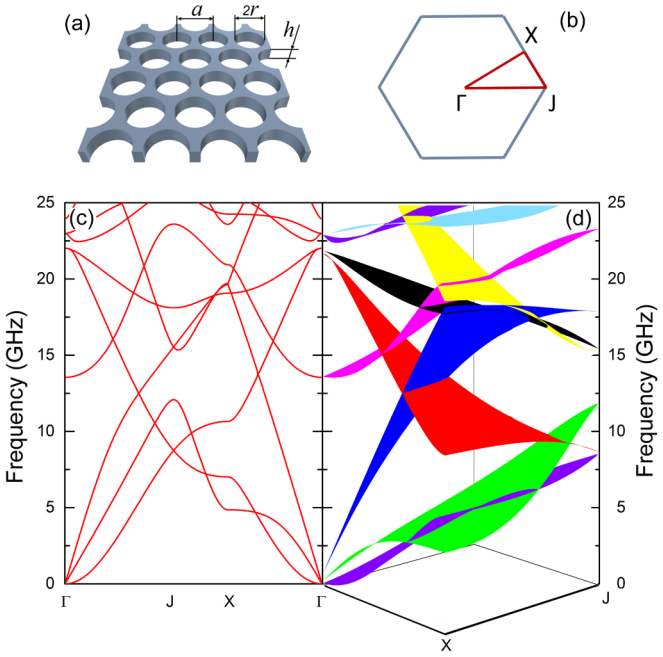

FIG. 1. (Color online) (a) Scheme of a typical phononic-crystal structure with (b) its first BZ. (c) Unsorted band diagram of the structure with $a = 160$ nm, $r/a = 0.4$, and $h = 80$ nm plotted at the periphery of the irreducible triangle of the first BZ and (d) sorted band diagram plotted in the interior of the irreducible triangle of the first BZ.

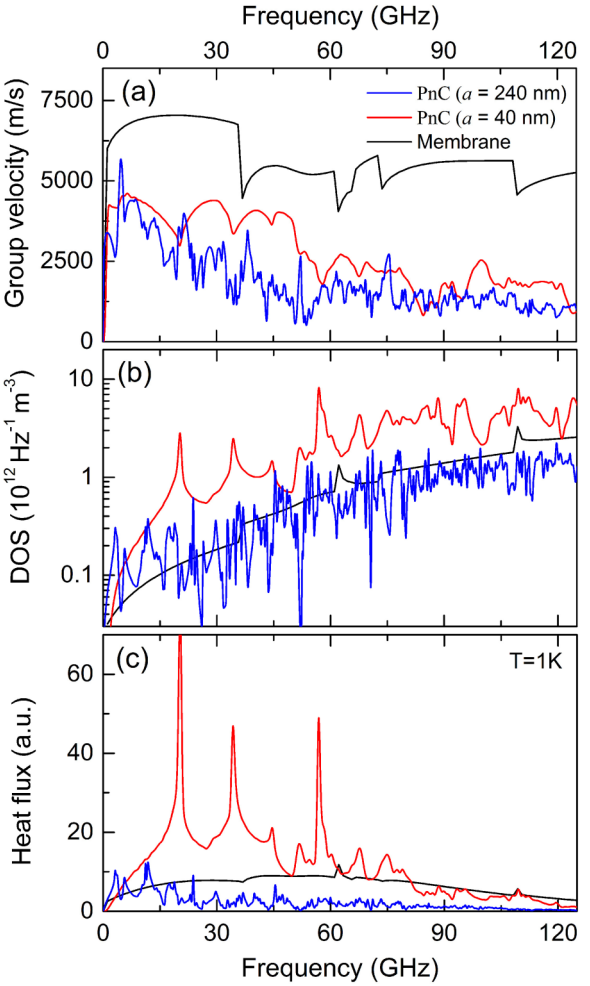

FIG. 2. (Color online) Spectra of (a) the average group velocity, (b) the DOS, and (c) the power flux at 1 K calculated for the membrane and phononic structures with different periods ($a = 40$ nm in red and $a = 240$ nm in blue) and $r/a = 0.4$ for both structures. Thickness of the membrane and phononic structures is 80 nm.

used analytic Rayleigh-Lamb equations [18]. In this case, dispersion does not require sorting and interpolation, which provides an opportunity to estimate the maximum error that may be caused by these two operations. For this purpose, we compared the heat flux calculated from the analytically obtained dispersion relation of a membrane to that calculated from the dispersion obtained numerically by COMSOL MULTIPHYSICS®. The difference between these values was found to be about 15%, which reflects the maximal potential error of this calculation. To further verify the validity of our calculation we simulated the same structures as those studied in the literature [5,6,16,19,20] and found good agreement with obtained band diagrams and spectra of both group velocity and DOS. The slight differences can be explained by the fact that the planar-wave expansion method, widely used in the literature for band diagram computation, is known to give less accurate results as compared to the FEM [21].

To illustrate the impact of phononic-crystal design on phonon properties we study two nanostructures of the same thickness (80 nm) and r/a ratio (0.4) but different periods ($a = 40$ and $a = 240$ nm). Let us consider the group velocity and the DOS spectra of these structures. Due to van Hove singularities these spectra show much stronger fluctuations than corresponding spectra of the membrane. The group velocities of both phononic structures are reduced in comparison to that of an unpatterned membrane due to the band flattening but do not significantly differ one from another [Fig. 2 (a)]. Indeed, on one hand the phonon modes are flattening as the period is increased [5], but on the other hand the size of the first BZ is inversely proportional to the period, so the $d\omega/dk$ ratio remains approximately the same. As for the DOS, although the structure with $a = 240$ nm shows values that are comparable to those of the membrane, the structure with $a = 40$ nm demonstrates significantly higher DOS values [Fig. 2(b)]. This change in the DOS originates from the difference in the size of the first BZ: The shorter the period, the larger the size of the first BZ and the longer the length of the constant frequency in k space. This, together with the nearly constant group velocity, results in the higher DOS [see Eq. (1)]. This implies that more phonons can exist in the structures with lower periods. As a consequence, the structure with $a = 240$ nm shows a reduction in its heat flux spectrum as compared to the membrane, whereas the structure with $a = 40$ nm, on the contrary, shows an enhancement, at least in the 3–80-GHz range [Fig. 2(c)]. Above 80 GHz the group velocity of the phononic structure is getting low and compensates high DOS. At very low frequencies, on the contrary, the heat flux is decreased due to the low DOS despite the high group velocity. The highest peaks of the heat flux spectra correspond to the van Hove singularities of the first few modes at the edge of

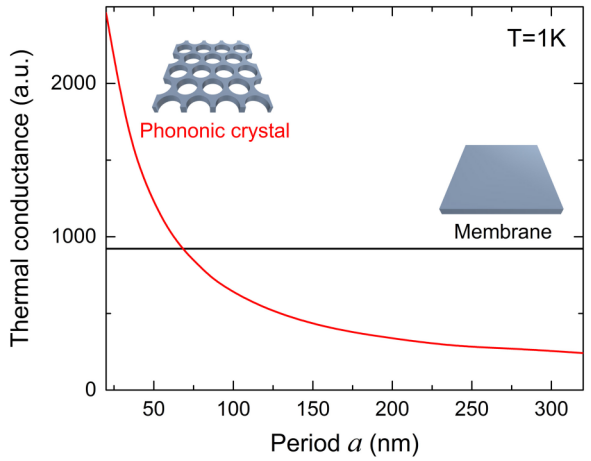

FIG. 3. (Color online) The thermal conductance of the membrane and phononic crystals as a function of period a ($r/a = 0.4$ and $h = 80$ nm) calculated at 1 K.

the first BZ. Note that at these points even the heat flux of the structure with $a = 240$ nm exceeds that of the membrane.

To demonstrate the dependence of this effect on the period of the structure, we evaluate the integral of the heat flux up to the highest available states at a given temperature: $G(T) = \int Q(\omega,T)d\omega$. This quantity is proportional to the thermal conductance of the structure. Figure 3 shows the relative values of thermal conductance as a function of period at the temperature of 1 K. Structures with a period above 70 nm demonstrate a reduction in thermal conductance as compared to the membrane, but those with the period below 70 nm show higher values than the membrane. This counterintuitive result implies that, despite the presence of air holes and consequently smaller volume of the material, certain phononic structures are more conductive than an unpatterned membrane.

It is important to note that the effect discussed in this paper is relevant only at temperatures at which the dominant phonon wavelengths are comparable to the characteristic size of the structure (i.e., not above several Kelvin for realistic nanostructures) [10]. Indeed, this wave-property-based approach shows excellent agreement with experimental results only at sub-Kelvin temperatures [5]. This also indicates that at the low-temperature limit the phonon transport is mostly controlled by coherent scattering, whereas incoherent scattering mechanisms, which can mask this effect, play a negligible role. At room temperature it is unlikely that the periodicity affects the thermal transport of realistic nanostructures because the phonon wavelength in bulk silicon is on the order of several nanometers [22]. In addition, the thermal conductance is significantly impacted by temperature due to the Bose-Einstein distribution, which, depending on the temperature, allows occupation of only a limited number of the first bands. For these reasons, it is important to consider the temperature dependence of this effect.

Figures 4(a) and 4(b) show the heat flux spectra in a phononic crystal ($a = 80$, $h = 80$ nm, and $r/a = 0.4$) and an unpatterned membrane ($h = 80$ nm) at 2 and 0.1 K, correspondingly. At 2 K most of the phononic-crystal spectrum, except for the low-frequency part, lies below that of a

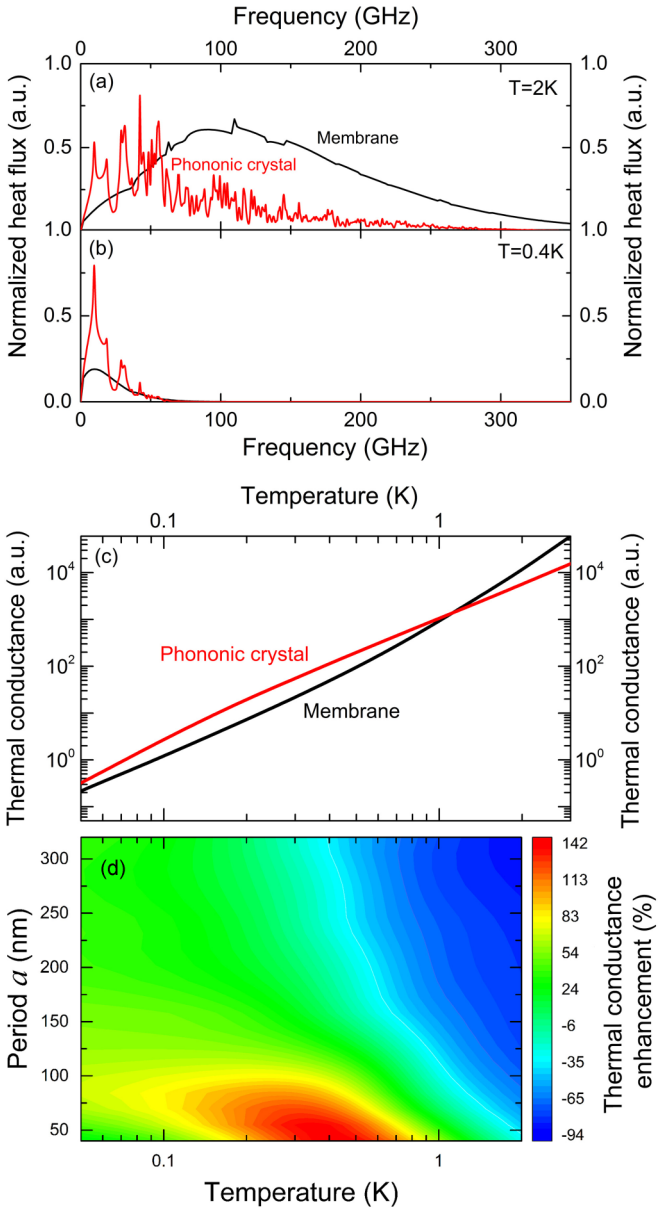

FIG. 4. (Color online) Heat flux spectra in a phononic crystal ($a = 80$, $h = 80$ nm, and $r/a = 0.4$) and an unpatterned membrane ($h = 80$ nm) at (a) 2 K and (b) 0.4 K. (c) The thermal conductance in the phononic structure and the membrane as a function of temperature. (d) Relative enhancement of thermal conductance in phononic structures as compared to the membrane plotted as a function of temperature and period.

membrane, which reflects the case of the thermal conductance reduction. At 0.4 K, the spectrum is limited by the Bose-Einstein distribution to the first 50 GHz, resulting in the dominant contribution coming from the low-frequency part of the spectrum. In this case, the spectrum of the phononic crystal clearly exceeds that of the membrane, which corresponds to the case of a thermal conductance boost. To demonstrate the transition between these two cases, Fig. 4(c) shows the temperature dependence of the thermal conductance in the phononic crystal and the membrane. For the given phononic crystal, the transition from the reduction in thermal conductance to

its enhancement takes place at temperatures below 1 K. This shows that the phenomena of reduction and enhancement of thermal conductivity may be controlled not only by the design of the structure, but also by temperature. However, taking into account the period dependence of thermal conductance, the transition temperature must depend on the period of the structure. To provide a guideline for the experimental observation of this effect we provide the map of the relative enhancement of thermal conductance in phononic structures as compared to the membrane $\Delta G = (G_{\mathrm{PnC}} - G_{\mathrm{Mem}})/G_{\mathrm{Mem}}$, plotted as a function of both the temperature and the period [Fig. 4(d)]. The map shows that the greatest enhancement of thermal conductance (red color) is observed in the area where both the temperature and the period are relatively low. However, for any given period there exist low enough temperatures where the enhancement can be observed. Indeed, even in the structures with long periods the heat flux exceeds that of the membrane at the points where the first few modes reach the edge of the first BZ [see Fig. 2(c)]. Yet, even for very short periods, the strongest enhancement is observed only in a certain range of temperatures, and below this range the enhancement is weakening again. This feature is explained by relatively low values of the DOS at the very low frequencies: Phonons can occupy only the first three modes near the center of the first BZ where the number of states is low (see Figs. 1 and 2).

To summarize, we have demonstrated that the efficiency of phonon transport in phononic crystals may not only be reduced as compared to an unpatterned membrane, but also, under certain conditions, enhanced. This enhancement originates from the increase of the DOS and relatively high group velocities of low-frequency phonons. This thermal conductance boost effect appears in the phononic crystals with periods below certain values and increases as the period is decreased. Moreover, this effect is significantly impacted by temperature, to the extent that there exist low enough temperatures at which structures with any period are expected to exhibit an enhancement of thermal conductance.

ACKNOWLEDGMENTS

This work was supported by the Project for Developing Innovation Systems of the Ministry of Education, Culture, Sports, Science and Technology (MEXT), Japan, Kakenhi (Grants No. 2570909 and No. 15K13270), and the Foundation for the Promotion of Industrial Science.

[1] G. Schierning, Phys. Status Solidi **211**, 1235 (2014).
[2] M. Maldovan, Nature (London) **503**, 209 (2013).
[3] J. Gomis-Bresco, D. Navarro-Urrios, M. Oudich, S. El-Jallal, A. Griol, D. Puerto, E. Chavez, Y. Pennec, B. Djafari-Rouhani, F. Alzina, A. Martínez, and C. M. S. Torres, Nat. Commun. **5**, 4452 (2014).
[4] M. Nomura and J. Maire, J. Electron. Mater. **44**, 1426 (2014).
[5] N. Zen, T. A. Puurtinen, T. J. Isotalo, S. Chaudhuri, and I. J. Maasilta, Nat. Commun. **5**, 3435 (2014).
[6] E. Dechaumphai and R. Chen, J. Appl. Phys. **111**, 073508 (2012).
[7] P. E. Hopkins, C. M. Reinke, M. F. Su, R. H. Olsson, E. A. Shaner, Z. C. Leseman, J. R. Serrano, L. M. Phinney, and I. El-Kady, Nano Lett. **11**, 107 (2011).
[8] B. L. Davis and M. I. Hussein, Phys. Rev. Lett. **112**, 055505 (2014).
[9] J.-K. Yu, S. Mitrovic, D. Tham, J. Varghese, and J. R. Heath, Nat. Nanotechnol. **5**, 718 (2010).
[10] A. Jain, Y.-J. Yu, and A. J. H. McGaughey, Phys. Rev. B **87**, 195301 (2013).
[11] J. Tang, H.-T. Wang, D. H. Lee, M. Fardy, Z. Huo, T. P. Russell, and P. Yang, Nano Lett. **10**, 4279 (2010).
[12] Q. Hao, G. Chen, and M. S. Jeng, J. Appl. Phys. **106**, 114321 (2009).
[13] T. Y. Hsieh, H. Lin, T. J. Hsieh, and J. C. Huang, J. Appl. Phys. **111**, 124329 (2012).
[14] M. Nomura, J. Nakagawa, Y. Kage, J. Maire, D. Moser, O. Paul, M. Nomura, J. Nakagawa, Y. Kage, J. Maire, and D. Moser, Appl. Phys. Lett. **106**, 143102 (2015).
[15] M. Nomura, Y. Kage, J. Nakagawa, T. Hori, J. Maire, J. Shiomi, R. Anufriev, D. Moser, and O. Paul, Phys. Rev. B **91**, 205422 (2015).
[16] R. Pourabolghasem, A. Khelif, S. Mohammadi, A. A. Eftekhar, and A. Adibi, J. Appl. Phys. **116**, 013514 (2014).
[17] J. P. Srivasatava, *Elements of Solid State Physics* (PHI Learning Pvt. Ltd., Delhi, 2014).
[18] T. Kühn, D. V. Anghel, J. P. Pekola, M. Manninen, and Y. M. Galperin, Phys. Rev. B **70**, 125425 (2004).
[19] S. Mohammadi, A. A. Eftekhar, A. Khelif, H. Moubchir, R. Westafer, W. D. Hunt, and A. Adibi, Electron. Lett. **43**, 898 (2007).
[20] J. O. Vasseur, P. A. Deymier, B. Djafari-Rouhani, Y. Pennec, and A. C. Hladky-Hennion, Phys. Rev. B **77**, 085415 (2008).
[21] M.-C. Lin and R.-F. Jao, Opt. Express **15**, 207 (2007).
[22] K. Esfarjani, G. Chen, and H. T. Stokes, Phys. Rev. B **84**, 085204 (2011).